Hydrogen separation by thin vanadium-based multi-layered membranes

Stefano Fasolin,[a] Simona Barison,*[a] Stefano Boldrini,[a], Alberto Ferrario,[a] Matteo Romano,[a,b] Francesco Montagner,[a] Enrico Miorin,[a] Monica Fabrizio,[a] and Lidia Armelao[a,b]

[a] Institute of Condensed Matter Chemistry and Technologies for Energy (ICMATE), National Research Council of Italy (CNR), Corso Stati Uniti 4, 35127 Padova, Italy
E-mail: simona.barison@cnr.it

[b] Dept. Chemical Science, University of Padua, Via Marzolo 1, 35131, Padova, Italy

Abstract

Thanks to their high hydrogen permeability, vanadium based alloys can be a valuable and sustainable alternative to palladium alloys, commonly employed in commercial membranes for hydrogen purification/separation. In this work, the unprecedented deposition of micrometric vanadium-based multilayers and their investigation as hydrogen selective membranes have been reported. In particular, this work describes the use of High Power Impulse Magnetron Sputtering, a technique easily scalable also for other geometries as tubes, for the deposition of dense and crystalline Pd/$V_{93}Pd_7$/Pd multilayers, with total thickness < 7 µm, onto porous alumina. These membranes showed high hydrogen fluxes in the 300-400°C temperature range, up to 0.26 mol m^{-2} s^{-1} at 300 kPa pressure difference and 375°C, as well as an unexpected and significant resistance to hydrogen embrittlement and to syngas in operating conditions.

Keywords: Vanadium • Hydrogen • Membrane • High Power Impulse Magnetron Sputtering • Multilayer

Introduction

Hydrogen-based energy systems are an attractive strategy for a future replacement of the current fossil fuel-based systems. In fact, H_2, with its high energy density (33 kWh/kg), is a valuable energy vector that can increase penetration of renewable and intermittent sources.[1]

At industrial scale, 95% of hydrogen is currently produced in the United States by steam reforming of natural gas,[2] but hydrogen production from biomass gasification can still accelerate the utilization of H_2 as a sustainable fuel for the future.[3,4] In steam reforming or biomass gasification reactors, an H_2-rich gas mixture containing CO, CO_2 and other by-products such as H_2S and NH_3 is obtained. Therefore, to produce pure H_2 some chemical processes are carried out in a number of reaction units followed by separation/purification (mostly by pressure swing adsorption).[5]

The large number of steps to produce and separate hydrogen affects the whole process in terms of system efficiency and costs, but the specific limits of traditional reactors can be circumvented by using integrated systems such as membrane reactors,[5] in which both reaction and separation are carried out in the same device. In fact, membrane technology is nowadays increasingly considered as a candidate for substituting conventional purification systems, thanks to several advantages including low energy consumption, ability to carry out separation continuously, and simple scaling up.[6] However, this technology will become attractive only when membranes will achieve some targets as suitable hydrogen flux, cost, durability and tolerance to pollutants.[7-9]

Since most of commercial membranes are based on palladium and its alloys, a cost reduction and an increase in membrane sustainability can be fulfilled only by using an alternative metal to Pd, or by limiting the use of Pd to few % or to very thin

surface layers. Several metals belonging to the groups IV and V and not included among critical elements show high hydrogen permeability and have been studied as possible alternatives to Pd.[8,9-14] In particular, the rate of hydrogen transport through the lattice of group V metals is typically an order of magnitude higher than through any other metallic lattice including palladium.[15]

Among the group V metals, the high hydrogen solubility of vanadium at pressures of practical interest may affect its mechanical stability due to embrittlement. For limiting the hydrogen solubility, various binary and ternary alloys of vanadium have been tested, and Pd was identified as one of the most efficient alloying element in substitutional alloys.[8-17] In particular, $V_{90}Pd_{10}$ and $V_{92.7}Pd_{7.3}$ resulted promising, demonstrating an optimal permeability to hydrogen and relativity good ductility.[16-18] In fact, alloying with Pd reduces the hydrogen solubility of pure vanadium to ranges of pressure and concentration that are more advantageous for practice ($P > 0.1$ MPa and [H]/[M] between 0.1 and 0.2).[17] Since the phase diagram of the V-Pd system shows several intermetallics, the amount of Pd should not exceed 18 at% to guarantee a solid solution.

Most commercial purification units contain conventional metal membranes consisting of relatively thick (>20 μm) Pd-alloy sheets or tubular membranes. However, to further reduce the noble metal content, an effective strategy is to reduce dense membranes to few μm films deposited on suitable porous substrates. Various Pd- and Pd alloys-based membranes have been produced and tested as few μm films deposited onto porous alumina, nickel or stainless steel,[19] but they still lack of sufficient long-term stability and selectivity. Conversely, to the best of our knowledge, so far vanadium or vanadium alloys membranes have been tested only as sheets or tubes with thicknesses ≥ 40 μm,[16,20] showing problems due to hydrogen embrittlement. These membranes need a protective coating against oxidation and palladium is typically used with the further function of catalytic layer for hydrogen absorption/desorption.[8,16] The Pd films, electroless deposited onto these membranes, showed some failures due to their delamination or Pd interdiffusion with the underlying alloy.[16,21,22]

Conversely to electroless plating, magnetron sputtering is effective in depositing alloys with variable compositions;[23] it also allows the sequential deposition of protective and catalytic Pd layers and of non-noble alloys in one stage in vacuum, thus avoiding the oxidation at the interface. In this work, we exploited for the first time a recent evolution of this technique, the High Power Impulse Magnetron Sputtering (HiPIMS), for the deposition of a hydrogen-selective membrane film.

HiPIMS, introduced by Kouznetsov et al. in 1999,[24] is a successful technique for improving magnetron sputtering by pulsed power technology. Its main feature is the combination of sputtering from standard magnetrons using pulsed plasma discharges, with the aim of generating highly ionized plasma with large quantities of ionized sputtered material.[25] The high degree of ionization of the sputtered species, combined to a bias voltage applied to the substrate, has been shown to lead to the growth of smooth and dense films, to enable a good control on composition and microstructure, and to improve film adhesion and uniformity also on complex shapes.[26]

In this work, the $V_{93}Pd_7$ composition was chosen to limit the Pd content, to avoid intermetallics formation and since a similar alloy exhibited hydrogen permeability higher than a typical commercial Pd–Ag alloy.[18] $Pd/V_{93}Pd_7/Pd$ multilayer films, with total thickness <7 μm, were deposited by a combined HiPIMS/Direct Current (DC) magnetron sputtering process onto porous alumina.

Since porous substrates can significantly affect the final cost of membranes, alumina has been chosen being an inexpensive material, mechanically and chemically stable in operating conditions. Alumina substrates present also the advantage of preventing interdiffusion phenomena at high temperatures, typical of steel substrates, an issue that can reduce hydrogen permeation. Therefore, a proper procedure has been set up to achieve substrates having a controlled porosity to allow the deposition of a dense metallic layer with no need of an interlayer.

The morphology, composition and structure of membranes were characterized and the hydrogen permeability was measured. Moreover, considering that still good result for V_xPd_y membranes in terms of resistance to hydrogen embrittlement and syngas have not been demonstrated so far, these aspects were deeply investigated.

Experimental Section

Materials and methods

Alumina-based porous supports have been prepared by mixing different ratios of α-Al_2O_3 powder (Alfa Aesar, 99.9% metal basis) and a pore former. Poly-methyl methacrylate powders (PMMA) with spherical shape and different average particle dimension (Soken Chemical & Engineering - average size 1.5 µm, 3 µm or 7 µm) were tested as pore former. A wet ball milling process (absolute ethanol, Sigma Aldrich ACS reagent ≥ 99.8%) in zirconia jars with proper amount of zirconia balls were carried out in a planetary mill (Fritsch Pulverisette 7) at 350 rpm for a total of 2 h for each mixture. Various ratios between Al_2O_3 and pore former were tested (20, 40, 50 and 65 vol% of PMMA).

As obtained mixtures were uniaxially pressed (Nannetti Mignon SS/EA) in a 2.5 cm diameter mold by a 140 MPa load. Thermogravimetric (SDT Q 600, TA Instrument) and dilatometric analyses (Netzsch DIL 402PC) were performed to develop the sintering process and to help in choosing ramps and holding times. The disks were sintered at 1500 °C in a high temperature furnace (Nabertherm HT 04/17), then polished and cleaned in an ultrasonic bath. The porosity was estimated by measuring the geometrical density and comparing it with the theoretical value of 3.98 g/cm^3 for alumina density.

The membranes were deposited by combined unbalanced HiPIMS/DC magnetron sputtering technique. Before depositions the chamber was evacuated to a base pressure ≤1x10^{-4} Pa, while depositions were conducted in Argon atmosphere (Ar, 99.999% purity) at 1 Pa. During depositions the substrates were rotated at 5 rpm to improve homogeneity. Prior to alloy sputtering, a thin film of Pd was deposited onto alumina at room temperature by DC (100 W, 30 min deposition), to achieve also a conductive layer for a proper bias application during the following depositions. A co-sputtering process was developed for the VPd alloy deposition by virtue of a deep preliminary set-up of the process to properly regulate the power on vanadium and palladium targets to achieve the V 93at% - Pd 7at% composition. The vanadium target was powered by HiPIMS (Trueplasma HighPulse 4002, Hüttinger Electronic, Germany) at a mean power of 700 W (9 Wcm^{-2}, pulse length 30 µsec, frequency 500 Hz), while palladium target was powered by DC (Trueplasma DC 4001, Hüttinger Electronic, Germany) at 100 W (5 Wcm^{-2}). The distance substrate-target was set at 120 mm for V and 200 mm for Pd, to achieve the right composition. During depositions, the substrates were heated at 350 °C and a 100 V negative bias was applied (Trueplasma Bias 3018, Hüttinger Electronic, Germany). After alloy deposition, the power on vanadium target was switched off and the Pd deposition was continued for 30 min to produce a pure Pd thin film on the top surface.

Characterization

Structural and microstructural information on the crystalline phases of the membranes were obtained by XRD and Rietveld refinement. The patterns were recorded at room temperature using a Philips PW 1830 diffractometer with Bragg-Brentano geometry, employing a Cu anode X-ray tube operated at 40 kV and 30 mA (angular range from 30° to 100°, 0.02° step, 6 s per step). Rietveld refinements on X-ray powder diffraction patterns were performed using MAUD software.[27] Surface and fractured surfaces of samples were observed by field emission scanning electron microscopy (FE-SEM) with a SIGMA Zeiss instrument (Carl Zeiss SMT Ltd, UK), operating in high vacuum conditions at an accelerating voltage of 20 kV and the composition was determined by Energy Dispersive Spectroscopy (EDS, Oxford X-MAX, UK). The surface roughness of alumina substrates was measured by a mechanical profiler (KLA Tencor P10, USA).

Membrane permeability measurements were carried out by means of a custom-built stainless steel test station. A scheme of the permeation test apparatus is reported in Figure S1 in Supplementary Information (SI). Membranes were clamped and sealed in a stainless steel module using graphite gaskets. The module consists of two parts, feed side and permeate side, connected by a channel of about 1 cm in diameter, closed by the membrane to be tested, and placed in a furnace (Nabertherm N11/HR). The membrane housing temperature was monitored by a K-type thermocouple inserted directly in the module test. The gas flows at feed and permeate sides were set by independent mass flow controllers (1179A, 1179B and 647C, MKS). The pressure at the feed side was controlled by a Baratron pressure transducer (722B, MKS). Nitrogen and helium (99.999% purity) were used to test membrane selectivity, while high purity hydrogen was produced by an electrolyser (Perkin Elmer PGX Plus H2 160).

During permeability tests, the feed side pressure was varied from absolute pressures of 110 kPa to 400 kPa, while at permeate side was set at atmospheric pressure by a sweep gas flow. The gas flow in feed side was measured after reaching stationary conditions (flow fluctuations <1%). Pressure, flows and temperature were controlled and monitored by a

Labview interface. Prior to each permeation test, the hydrogen flux was stabilized and monitored for few hours to ascertain or achieve a stable flux (Figure S2 in SI reports an example). After reaching stationary conditions, the hydrogen permeation was measured in typical conditions used to test these membranes, that is at 5 temperatures, from 300 to 400 °C, and at 16 ΔP values, from 300 to 10 kPa (descending). For each pressure point, the value was recorded after reaching a stable flux and the permeance at different pressures was tested twice for each temperature. The measures were repeated for membranes deposited in the same conditions to verify repeatability. The selectivity was evaluated by the ratio between hydrogen and nitrogen permeances.

Results and Discussion

Alumina support

A major aspect on the development of selective membranes is the preparation of inexpensive, mechanically and chemically stable supports, with controlled porosity, to prevent pressure drops and to allow the deposition of dense films, without the need for interlayers. PMMA, previously employed to prepare porous ceramics,[28] was investigated as pore former. Thermogravimetric and dilatometric analyses were performed to identify the decomposition temperature, the pellet shrinkage and the proper heating ramp. The decomposition temperature of PMMA resulted centered at around 385 °C (thermo-grams not reported here). Various amounts of PMMA were tested, from 20 to 65 vol% with respect to alumina. Powders with different mean sizes were tested (1.5, 3 and 7 µm). The thermal characterization identified a suitable sintering treatment up to 1500 °C, with an isotherm step of 1 h at 385 °C and a very slow heating rate above 1000 °C (30 °C/h), when the shrinkage is maximum, to avoid pellet bending. With this procedure, planar and porous substrates were achieved. In particular, the pellets prepared with 65 vol% of 1.5 µm mean size PMMA powder resulted in substrates with ~2 cm diameter (20-25% shrinkage), porosity > 35%, homogenous pore size distribution (see Figure 1) and maximum surface pore size of about 0.5-0.6 µm. The mean surface roughness was 0.26 µm.

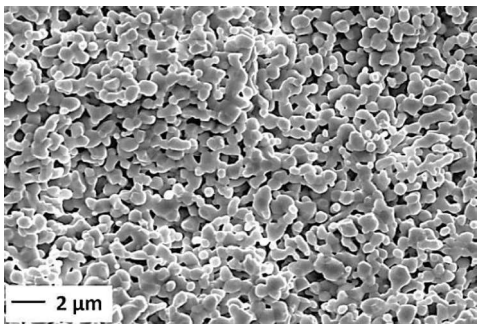

Figure 1. Cross-sectional view of alumina prepared with 65 vol% of PMMA (1.5 µm mean powder size).

H_2, He and N_2 fluxes through alumina substrates were measured to evaluate the influence of the substrate to membrane permeability and to measure mean pore size (Figure S3a in Supplementary Information, SI). According to the procedure reported in SI, a mean pore size of about 0.5 µm was estimated, a value compatible with the pore size shown by SEM analysis. The hydrogen flux in porous substrates (see an example at 400 °C in Figure S3b) was measured at various temperatures and for supports with different thickness. Considering typical fluxes measured for membranes, the porous substrates accounted for a pressure drop of at most 10-15 kPa for 1.2 mm thick substrates, and its influence was taken into account in membrane permeance estimation. The influence of the substrate thickness on hydrogen flux was also verified by measuring two membranes with the same metal multilayer and two substrates, 0.5 or 1.2 mm thick, which showed similar flux values within measurement uncertainty.

Multilayer deposition and characterization

For the accurate bias application during the next VPd alloy deposition, a first Pd layer was preliminarily deposited (room temperature, unbalanced DC, deposition rate 11-12 nm/min, Pd thickness 0.34 - 0.36 μm) in order to create a conductive layer.

HiPIMS/DC depositions of VPd alloy onto Pd/alumina substrates were then carried out for deposition times from 3 to 9 hours. Mean deposition rate of about 0.67 μm/h was calculated on thickness ranging from about 1.8 to 6 μm. The multilayer was then completed with a top layer of Pd (deposition time 30 min). A scheme of all samples investigated is reported in Table1.

Table 1. Scheme indicating the name and the thickness of all layers including alumina porous supports of all samples investigated.

Sample name	Multi-layer thickness (μm)	Pd film on top surface	$V_{93}Pd_7$ film	Pd film at interface	Alumina substrate
		Thickness (μm)	Thickness (μm)	Thickness (μm)	Thickness (μm)
M25	2.5	0.35	1.8	0.35	600
M42	4.2	0.35	3.5	0.36	1200
M57	5.7	0.35	5.0	0.35	1200
M67	6.7	0.34	6.0	0.35	500 or 1200

The manifold role of two Pd thin films in the final multilayer membranes was to prevent vanadium oxidation and interdiffusion phenomena, and to act as catalytic layers for hydrogen absorption/desorption.

SEM micrographs of the top surface of sample M67 (Figure 2) show the morphology of the outer palladium film, characterized by a very homogeneous, compact, dense and crystalline structure.

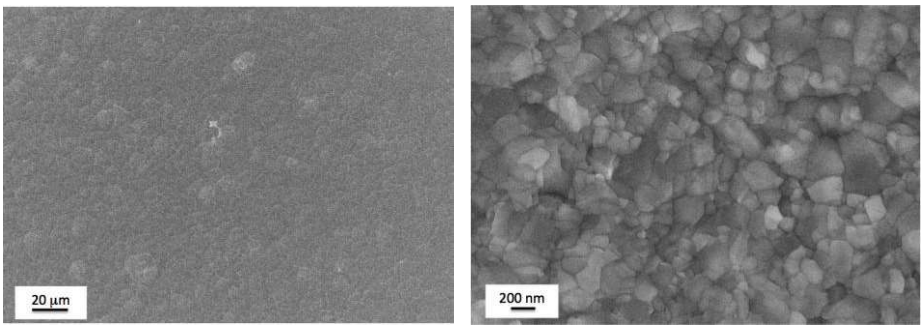

Figure 2. SEM micrographs at different magnifications of the Pd surface for the M67 sample.

Figure 3 shows a backscattered electron image and a scheme of the fracture of M42 sample. The micrograph highlights the Pd films on both sides of the alloy and shows a dense and compact VPd layer.

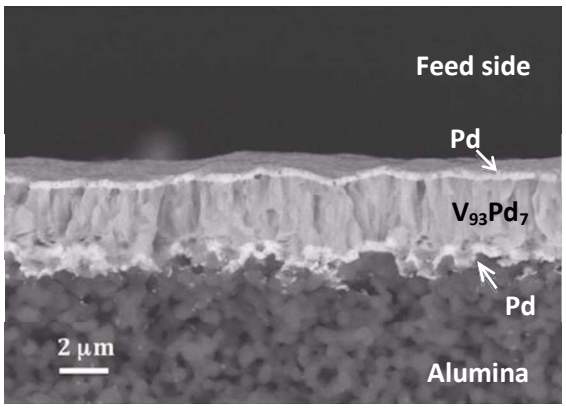

Figure 3. Cross-sectional view of the M42 specimen taken under backscattered electron mode.

The alloy composition was measured by EDS in all samples and was verified on a VPd layer deposited without Pd films, resulting in a mean composition of V 93.1 at% and Pd 6.9 at% (± 0.7 %), i.e. very close to the nominal value.
XRD analysis allowed investigating the crystalline nature of the as-deposited multi-layer membranes. Figure 4 reports, as an example, the XRD pattern recorded on the M67 sample. The pattern is very similar to that reported by Paglieri *et al.* for a $Pd/V_{90}Pd_{10}/Pd$ foil.[16] The Rietveld refinement identified the peaks due to the Pd thin films (cubic Fm-3m, cell parameter of 3.875 Å, mean crystallite size of ≈ 150 nm) and to the VPd alloy (cubic Im-3m, cell parameter of 3.020 Å, mean crystallite size of ≈ 190 nm), besides very week peaks due to alumina substrate.

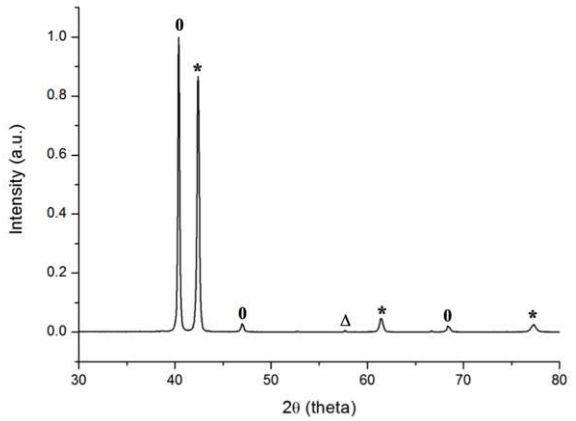

Figure 4. XRD pattern of the as-deposited M67 sample. * refers to VPd alloy, ^{0} to Pd thin film and Δ to alumina substrate peaks.

Hydrogen fluxes

The hydrogen fluxes were measured in all membranes in the 300-400 °C and 10-300 kPa ranges. Figure 5 reports the H_2 fluxes measured at various temperatures as a function of the pressure difference between feed and permeate side for samples M42 and M67. The flux values (up to 0.26 mol_{H_2} m^{-2} s^{-1} at ΔP = 300 kPa) are higher than those reported by Paglieri et al. for a Pd/V-10Pd 100 μm thick/Pd membrane,[16] and by Viano et al. for Pd/V/Ni or Pd/V/Pd membranes,[29] similar to those of a Pd(2 μm)/V(100 μm)/Pd(2 μm) membrane [21] or to a Pd/V 40 μm/Pd membrane,[30] and about a half of that of Pd(2 μm)/V(100 μm)/Pd(2 μm) membrane reported in [31]. The fluxes are similar to those of Pd or PdAg composites membranes.[32 and references therein]

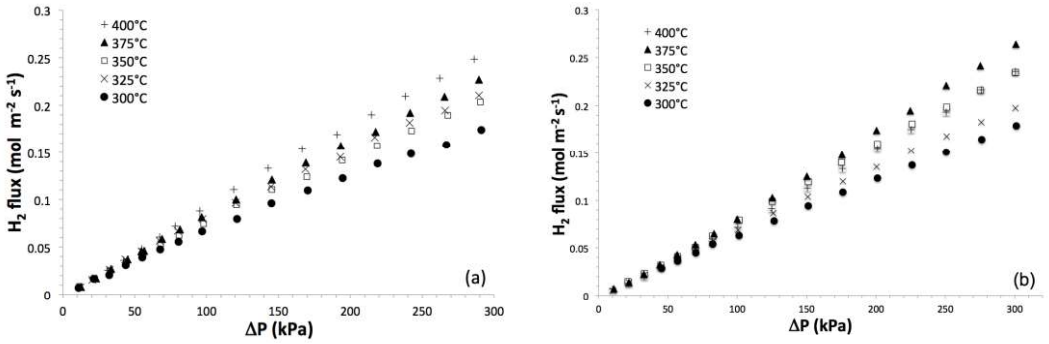

Figure 5. Flux measured between 300 and 400°C and as a function of the pressure difference between feed and permeate side in a) M42 and b) M67 membranes.

To compare membranes with different multilayer thickness, in Figure 6 are reported the fluxes measured at ΔP = 300 kPa as a function of temperature for all samples. The fluxes show an analogous trend with temperature, and the highest flux value of 0.26 mol m^{-2} s^{-1} is recorded for the M67 sample at 375 °C. The inset in Figure 6 shows the deviation of M25, characterized by a very high flux, i.e. > 0.7 mol m^{-2} s^{-1}. However, the selectivity of this sample, calculated as the ratio between hydrogen and nitrogen permeances, was low (~ 9 at all temperatures) and any trend with temperature was not ascertained. This behavior probably arises from the presence of pores/leaks in the multilayer structure due to the low thickness, which causes a Knudsen contribution to flow through pores.

By analyzing in more detail the trend of flux as a function of temperature, an increase of fluxes with temperature was observed for all samples with multilayer thickness > 2.5 µm (see as an example the diagram in Figure 7), with the exception of sample M67, where a decrease of flux was observed at 400 °C. By extrapolating the data at various temperatures from permeances calculated across the whole membrane at various pressures, apparent activation energies have comparable values for all samples, i.e. 10-12 kJ $mol_{H_2}^{-1}$. These values are consistent with typical values reported for the activation energy of hydrogen diffusion in vanadium.[8] In fact, the typical activation energy for diffusion-limited flow in Pd is estimated to be much higher (around 22-24 kJ mol_H^{-1}).[8,33]

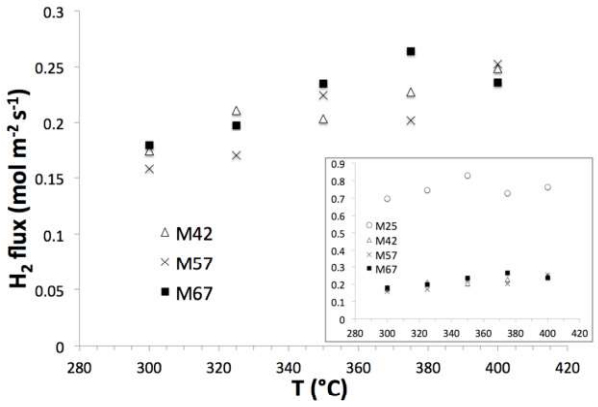

Figure 6. Flux values measured at ΔP = 300 kPa vs *T* for different samples.

Therefore, permeation seems kinetically controlled by the VPd layers instead of Pd thin films. Furthermore, the system does not seem strongly influenced by surface and interface phenomena. This is in agreement with the conclusions of Ward and Dao that deeply modeled the hydrogen permeation in palladium membranes.[33] They found that for thin membranes (1 µm) at temperatures higher than 300 °C the flux trend with temperature shows a diffusion-limited flow only slightly influenced by a desorption-limited process, and they identified significantly higher activation energies for absorption or desorption processes (>42 kJ mol_H^{-1}). However, considering a mass transfer resistance at low pressure side, typical for thin film deposited on porous supports, they found a significant reduction of fluxes and a trend with temperature that could explain the flux reduction observed at 400 °C for M67 sample. We could thus hypothesize a permeation process controlled

by a combination of diffusion-limited flux in VPd alloy and mass transfer resistance in the alumina support. However, in a multilayer system as in the present case, modeling of phenomena influencing the hydrogen permeation is quite complex.

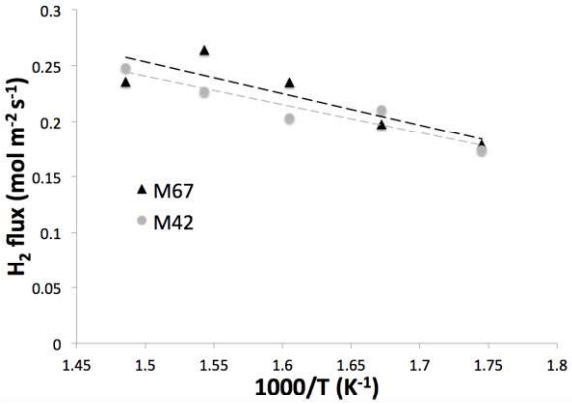

Figure 7. Fluxes measured at ΔP = 300 kPa vs 1000/T for samples M42 and M67.

Comparing with literature, in Pd/V-12.3Pd(160μm)/Pd membranes the permeation flux was found almost independent from temperature.[18] Conversely, an increase in permeability with temperature was also observed by Paglieri et al. for a Pd/V-10Pd(100 μm)/Pd membrane, and they observed activation energies, for permeances calculated with Sievert's law, of 12.9 kJ mol^{-1} only for temperatures ≥ 400 °C, and much higher (38.8 kJ mol^{-1}) at lower temperatures.[16]

Modeling the trend of flux with pressure in this system is also complex. Considering the Fick's first law to describe the atomic hydrogen diffusion through a homogeneous metal phase as a function of concentration gradient and diffusion coefficient, and the Sievert's law that may be used under certain conditions to describe the relationship between the concentration and pressure, equation (1) was derived to describe how the hydrogen flux (J) varies with temperature and pressure:[8]

$$J = \frac{\Phi}{L}\left(\sqrt{P_{feed}} - \sqrt{P_{perm}}\right) = \frac{\Phi_0 e^{\frac{Ea}{RT}}}{L}\left(\sqrt{P_{feed}} - \sqrt{P_{perm}}\right) \quad (1)$$

where Φ is the permeability, that is defined as the rate of gas permeation per unit area, per unit driving force (pressure in this case), per unit membrane thickness. E_a is the activation energy for the whole process, Φ_0 is the pre-exponential factor related to the permeability, R the gas constant, L the membrane thickness, P_{feed} and P_{perm} are the pressure at the feed and at the permeate sides, respectively. However, this equation is valid for thick membranes (commonly > 10 μm). Therefore, a more general formula has been typically used especially to estimate permeability or permeance (Φ/L) of thin palladium-based membranes, as in equation (2):[8]

$$J = \frac{\Phi}{L}\left(P^n_{feed} - P^n_{perm}\right) \quad (2)$$

Although limited, this formula is a general approach to take into account some phenomena that can lead to a best fit of flux data vs (P^n_{feed}-P^n_{perm}) with an exponent *n* higher than 0.5. Among them, there are surface resistance to H_2 absorption and desorption, mass transfer resistance in porous substrates, hydrogen diffusion as molecular H_2 along grain boundaries and/or Knudsen or viscous flow through pores and film defects and leaks.[8,34,35] In thin Pd membranes, *n* was shown to approach 1 and this was typically attributed to surface phenomena as the rate-limiting step.[36] In case of V-based membranes, hydrogen solubility was also taken into account and, although palladium in vanadium can reduce the hydrogen solubility in the alloy, a deviation from Sievert's law was observed in the pressure-composition isotherm for a bulk VPd alloy with 7.3 at% of Pd.[17]

For all samples (with multilayer thickness > 2.5 μm), an almost linear trend with ΔP (*n*=1) was observed (see Fig. 5). This behavior could be due to a combination of surface and interface controlled phenomena, hydrogen solubility in VPd alloy and mass transfer resistance in the porous supports at the low-pressure side. However, considering that the apparent activation energies were not significantly influenced by surface phenomena, the surface processes could not be the main

component of this deviation from Sievert's law. Taking into account the pressure-composition isotherms for hydrogen absorption in substitutional V-7.3Pd,[17] in case of diffusion-limited process the flux over VPd alloy could be estimated to be at least one order of magnitude higher than measured values. Therefore, the best fit with *n*=1 seems to confirm the hypothesis that flux in these membranes is predominantly controlled by a combination of a diffusion-limited process over the VPd alloy and a mass transfer resistance in the porous support, probably combined to some possible phenomena at the interfaces.

Figure 8 summarizes the data, showing fluxes and permeability values *vs* multi-layer thickness (the permeability values where calculated from eq. (2) considering *n*=1). The selectivity values are also reported as numbers in the graph, showing values of about 400 for multilayers with thickness ≥ 5.7 µm. This value corresponded to N_2 fluxes < $4x10^{-4}$ mol m^{-2} s^{-1} and is probably the limit of sealing system in our measurement apparatus. Even though we suppose that real selectivity is higher than these values, it is in most cases similar to values reported in literature for membranes based on films deposited by magnetron sputtering (see ref. [35] and references therein), although those films were deposited on mesoporous γ-Al_2O_3/α-Al_2O_3 or on substrates with surface porosity much finer that that reported in this work.

The permeability increases with the thickness of VPd layer and a maximum permeability of $6.3x10^{-12}$ mol_{H_2} m^{-1} s^{-1} Pa^{-1} was measured for M67 sample. This is probably due to the transition from a process controlled by interfaces and porous support to a process controlled by bulk diffusion in material.

A comparison with literature for V-based membranes is not correct since only foils with thickness ≥ 40 µm have been tested so far and data processed with Sievert's law and, if elaborated with Sievert's law the data of membranes reported in this manuscript would be much higher than literature data. However, the reported values of permeability, appropriately calculated as a function of ΔP, (and the corresponding permeances estimated around 7-$9x10^{-7}$ mol_{H_2} m^{-2} s^{-1} Pa^{-1}) are wholly in line with values reported for membranes based on thin Pd or PdAg films (with thickness ranging from 1 to 7 µm, see ref. [36] and references therein).

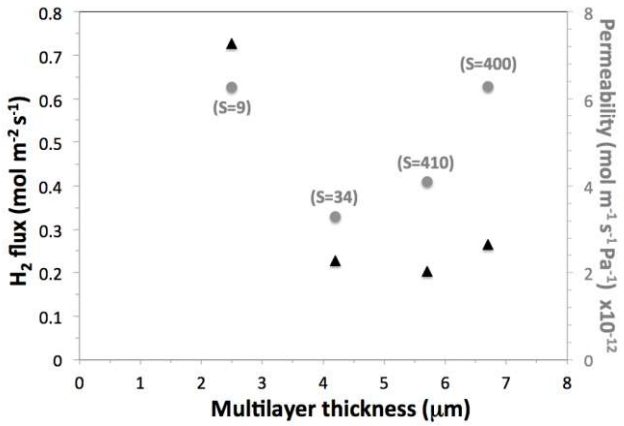

Figure 8. Fluxes measured at *ΔP* = 300 kPa and 375 °C and permeability values vs multi-layer thickness for all samples. The selectivity values (S) are reported as numbers in the graph.

Membrane stability

The main issue for real application of these membranes is the high hydrogen solubility and, as a consequence, failure due to embrittlement. Few works have been reported so far on the failure temperature and pressure of V-based membranes due to embrittlement and very rarely on stability of membranes deposited by magnetron sputtering. Paglieri et al. showed a failure temperature of 118 °C and a pressure failure of 97 kPa for a Pd/V-10Pd(100µm)/Pd membrane and of 262 °C and 97 kPa for a Pd coated 0.375 mm thick V membrane.[16] Wieland et al. showed a failure at about ΔP=300 kPa for a Pd/V(40 µm)/Pd membrane.[30]

In this study, all membranes have been tested for at least 2 weeks, at temperatures ranging from 300 to 400 °C and up to ΔP = 300 kPa, showing a stability in fluxes with time and no failure. For the M42 sample, a failure temperature onset seems to be below 100 °C at ΔP = 100 kPa and at about 200 °C at ΔP = 300 kPa (Figure S4). However, no abrupt increase of flux was ascertained, only a slight change in flux. In case of thicker multilayers, the failure temperature onset at ΔP = 300 kPa

seems at 200 °C (see Figure S5). The samples presented only few and small holes or cracks in the multi-layers after the tests down to room temperature.

To the best of our knowledge, vanadium-based membranes have never been tested in syngas or operating conditions. In this work, the M67 sample has been tested in commercial syngas (CO_2 15 mol%, CO 15 mol%, H_2 10 mol%, CH_4 3.025 mol% and N_2). In particular, the hydrogen flux was measured at 375 °C and ΔP = 300 kPa before and after various cycles of exposure to syngas (Figure 9).

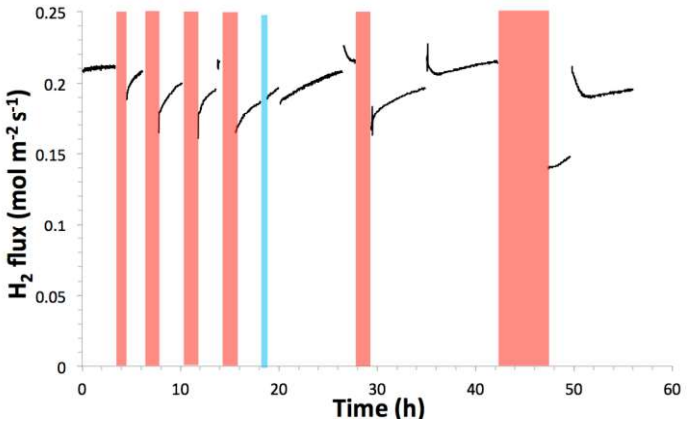

Figure 9. Hydrogen flux at 375 °C and ΔP = 300 kPa before and after various cycles of exposure to syngas (ΔP = 200 kPa) in a M67 sample. Red bars indicate the length of exposure to syngas (from 1 to 5 h), blue bar indicates the exposure to air (0.5 h), and the other changes in flux are due to exposure to nitrogen overnight.

The hydrogen flux decreased after exposure to syngas (of about 11% after 1 h up to about 35% after 6 h of continuous exposure), but was slowly recovered in hydrogen or nitrogen flux with a rate that diminishes with time of exposure to syngas. Such flux reduction is not due to induced film cracks or defects since an abrupt increase of flux was not observed and initial values were recovered (and no defects were observed nor changes in selectivity). The permeance decrease is not even caused by carbon formation on the film surface, since the flux was restored and it did not change after exposure to air. Therefore, a Pd surface reversible deactivation can be suggested, induced by CO absorption; when the membrane is exposed to H_2 or N_2 at 375 °C for a few hours his activity can be completely restored. Definitively, after a total exposure of 12 hours to syngas and after that to N_2, a hydrogen flux only few % lower than the initial flux was restored and the selectivity resulted unchanged.

The morphological characterization of membranes after permeability tests in hydrogen or after tests in syngas showed very similar results. SEM micrographs (Figure 10) indicated a homogeneous surface without any crack or delamination of the film. At high magnifications, nanometric holes are identified on the surface together with the presence of vanadium oxide, as determined by EDS, at the grain boundaries of the Pd film. The oxide presence at the grain boundaries was analogously identified after very short tests only in hydrogen or after long tests in hydrogen or syngas and did not vary with testing time.

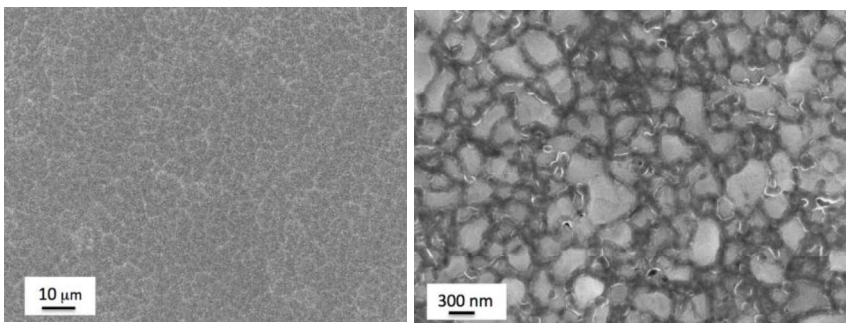

Figure 10. Surface SEM micrographs after permeability tests and syngas exposure of M67 sample.

The oxide presence is probably due to a slightly columnar structure of the Pd surface film, which was deposited by DC and not HiPIMS. The numerous cycles at high temperature during permeation tests probably enlarged the grain boundaries and

favored the vanadium diffusion along them. When exposed to air prior to SEM analyses, the vanadium at grain boundaries probably oxidizes.
XRD analysis (Figure S6) after permeation tests resulted in very similar spectra to those obtained for as-deposited samples, with the exception of a weak signal due to the presence of about 1.6 wt% of V_2O_3. It is worth noticing as this quantity does not change significantly with operating time. Cross-section SEM micrographs (not reported here) were very similar to those recorded before testing; only a very superficial (few nm) nano-porosity of the Pd top film was evidenced.

Conclusions

The deposition of thin vanadium-based membranes onto porous alumina substrates by a combined HiPIMS/DC technique was successfully performed. Membranes made by inexpensive, porous and stable alumina supports and metallic dense and crystalline $Pd/V_{93}Pd_7/Pd$ multilayers, up to 7 μm thick, have been prepared and tested. Membranes thicker than 4.2 μm showed suitable permeability and selectivity values and their permeability was very close to that of Pd membranes. Considering the mean Pd price in July-August 2017 and its amount in the membranes, the metal costs can be estimated lower than 450 €/m^2, that is compatible with commercial targets,[8] if considering also the ease in scaling up the HiPIMS deposition technique.
The resistance to hydrogen embrittlement at temperatures higher than 200 °C and up to ΔP of 300 kPa was also demonstrated. Moreover, the resistance to syngas was measured for the first time in vanadium-based membrane and a satisfactory stability was evidenced.
All these results indicate these membranes as a valuable and sustainable alternative to palladium-based membranes. The architecture of the membrane could be still improved e.g. by changing the composition of the VPd alloy and/or the composition, microstructure or thickness of the two thin Pd coatings, to improve the reported results.

Acknowledgements

The authors are grateful to Dr. Rosalba Gerbasi (CNR ICMATE) for XRD analyses and to Dr. Alessia Famengo (CNR ICMATE) for TGA analyses. This work has been founded by the MiSE-CNR Agreement “Ricerca di Sistema Elettrico 2015-2017”.

References

[1] R. Derwent, P. Simmonds, S. O'Doherty, A. Manning, W. Collins, D. Stevenson, *Int. J. Nuclear Hydrogen Production Application*, **2006**, *1*, 57-67.

[2] http://energy.gov/eere/fuelcells/hydrogen-resources

[3] S.E Hosseini, M. Abdul Wahid, M.M. Jamil, A.A.M. Azli, M.F. Misbah, *Int. J. Ener. Res.,* **2015**, *39*, 1597-1615.

[4] A. Demirbas, *Ener. Source Part A*, **2008**, *30(5),* 475-482.

[5] F. Gallucci, E. Fernandez, P. Corengia, M. Annaland, *Chem. Eng. Sci.,* **2013**, *92*, 40-66.

[6] N.A. Al-Mufachi, N.V. Rees, R. Steinberger-Wilkens, *Renew. Sust. Energ. Rev,* **2015,** *47*, 540-551.

[7] M. Sjardin, K.J. Damen, A.P.C. Faaij, *Energy* **2006**, *31*, 2523-2555.

[8] J.W. Phair, R. Donelson, *Ind. Eng. Chem. Res*., **2006**, *45(16),* 5657-5674.

[9] M.D. Dolan, *J. Membrane Sci.,* **2010**, *362(1-2),* 12-28.

[10] T. Osaki, Y. Zhang, M. Komaki, C. Nishimura, *Int. J. Hydrogen Energy,* **2003***, 28,* 297-302.

[11] M.D. Dolan, K.G. McLennan, G.Song, D.Liang, M.E.Kellam, *J. Membrane Sci*., **2013**, *446*, 405-409.

[12] M.D. Dolan, M.E. Kellam, K.G. McLennan, D. Liang, G. Song, *Int. J. Hydrogen Energy*, **2013**, *38*, 9794-9799.

[13] K.H. Kim, H. C. Park, J. Lee, E. Cho, S.M. Lee, *Scripta Materialia,* **2013***, 68,* 905–908.

[14] M. Matsuka, M. Higashi, T. Ishihara, *Int. J. Hydrogen Energy,* **2013**, 38, 6673-6680.

[15] T.S. Moss, N.M. Peachey, R.C. Snow, R.C. Dye, *Int. J. Hydrogen Energy*, **1998**, *23(2),* 99-106.

[16] S.N. Paglieri, J.R. Wermer, R.E. Buxbaum, M.V. Ciocco, B.H. Howard, B.D. Morreale, *Energy Materials,* **2008**, *3(3),* 169-176.

[17] V.N. Alimov, A.O. Busnyuk, M.E. Notkin, E.Y. Peredistov, A.I. Livshits, *Int. J. Hydrogen Energy*, **2014**, *39(34),* 19682-19690.

[18] V.N. Alimov, A.O. Busnyuk, M.E. Notkin, E.Y. Peredistov, A.I. Livshits, *J. Membrane Sci.*, **2015**, *481*, 54-62.

[19] S. Yun, S.T. Oyama, *J. Membrane Sci*., **2011**, *375***,** 28-45.

[20] H. Yukawa, T. Nambu, Y. Matsumoto, *J. Alloys Compd.*, **2011**, *509*, S881-S884.

[21] V.N. Alimov, A.O. Busnyuk, M.E. Notkin, A.I. Livshits, *J. Membrane Sci.*, **2014**, *457*, 103-112.

[22] D.J. Edlund, J. McCarthy, *J. Membrane Sci.*, **1995**, *107*, 147-153.

[23] T.A. Peters , M. Stange, R. Bredesen, in *Palladium Membrane Technology for Hydrogen Production, Carbon Capture and Other Applications*, 2015, Elsevier.

[24] V. Kouznetsov, K. Macák, J.M. Schneider, U. Helmersson, I. Petrov, *Surf. Coat. Tech*., **1999**, *122*, 290-293.

[25] K. Sarakinos, J. Alami, S. Konstantinidis, *Surf. Coat. Tech.,* **2010**, *204*, 1661-1684.

[26] D. Lundin, K. Sarakinos, *J. Mater. Res*., **2012**, *27(5),* 780-792.

[27] L. Lutterotti, S. Mattheis, H. R. Wenk, *Proc. Twelfth International Conference on Textures of Materials (ICOTOM-12),* **1999**, *1*, 1599.

[28] L. Mingyi, Y. Bo, X. Jingming, C. Jing, *Int. J. Hydrogen Energy*, **2010**, *35(7),* 2670-2674.

[29] D.M. Viano, M.D. Dolan, F. Weiss, A. Adibhatla, *J. Membrane Sci.*, **2015**, *487*, 83-89.

[30] S. Wieland, T. Melin, A. Lamm, *Chem. Eng. Sci*., **2002**, *57***,** 1571-1576.

[31] V.N. Alimov, A.O Busnyuk, M.E. Notkin, A.I. Livshits, *Technical Phys. Lett..*, **2014**, *40*, 228-230.

[32] S.K. Ryi, J.S. Park, S.H. Kim, D.W. Kim, K.I. Cho, *J. Membrane Sci*., **2008**, *318*, 346-354.

[33] T.L. Ward, T. Dao, *J. Membrane Sci.,* **1999**, *153***,** 211-231.

[34] B.D. Morreale, M.V. Ciocco, R.M. Enick, B.I. Morsi, B.H. Howard, A.V. Cugini, K.S. Rothenberger, *J. Membr. Sci.* **2003**, *212(1-2*), 87-97.

[35] F. Guazzone, Y. H. Ma, *AiCHE Journal*, **2008**, *54*, 487-492.

[36] T. Maneerung, K. Hidajat, S. Kawi, *J. Membrane Sci.* **2014**, *452*, 127-142.